Postprint of: Applied Clay Science 168: 106-115 (2019)

Cationic and anionic clay nanoformulations of imazamox for minimizing environmental risk

Rachid Khatem[a], Rafael Celis[b], M. Carmen Hermosín[b,*]

[a] *Laboratory of Biodiversity and Conservation of Soil and Water, University of Abdelhamid Ibn badis Mostaganem, Algeria*

[b] *Instituto de Recursos Naturales y Agrobiología de Sevilla, Consejo Superior de Investigaciones Científicas (IRNAS, CSIC), Spain*

*Corresponding author: M. Carmen Hermosín

Instituto de Recursos Naturales y Agrobiología de Sevilla (IRNAS, CSIC)

Avenida Reina Mercedes 10, 41012 Sevilla, Spain

E-mail: mchermosin@irnase.csic.es

Abstract

A synthesized anionic clay (layered double hydroxide or LDH) and a commercial cationic organoclay (Cloisite10A, Clo10A) were assayed as host nanocarriers for imazamox (Imz) herbicide. Imz-LDH complexes were obtained by direct synthesis (DS) and regeneration (RE), whereas Imz-Clo10A complexes were prepared by ground mixing (GM) and through methanol addition (weak [WC] and strong [SC] complexes). Characterization of the complexes showed that Imz was partially hosted in the interlayer structure of the resulting nanoherbicides, as anion or as neutral molecule, with some of the herbicide at the external surfaces, depending on the carrier and preparation. The nanoherbicides showed a total water release from 73 (Imz-LDH DS) to 98% (Imz-Clo10A GM) with an immediate release from 67 (Imz-LDH DS) to 93% (Imz-Clo10A GM), while technical Imz released instantaneously >98%. The herbicide maximum concentration in the leachates from Imz-treated soil columns decreased between 20 and 35% for nanoherbicides with respect to the technical Imz, and between 10 and 30% with respect to a commercial Imz formulation. Total herbicide soil leaching losses were reduced from 96 or 90%, for technical and commercial Imz, to 77-67% for nanoherbicides. Bioassays showed similar efficacy for nanoherbicides and commercial product. The diverse Imz-clay complexes are revealed as smart delivery systems for this systemic herbicide by decreasing Imz water pollution risk while maintaining efficacy, with the advantages of their soil compatible matrix and the possibility to be located at action point in the subsoil.

Keywords: Formulation; Pesticide; Pollution; Soil; Transport; Water

Introduction

Pesticides are chemicals widely used in modern agriculture to protect crops against pests and they are fully essential to sustain world population food security. However, the pesticide action is not limited to the intended target; pesticides also produce collateral non-desirable ecological, environmental, and even human health effects. Only a fraction of the applied pesticide reaches the target; the rest is distributed in the environment, mainly in the soil, where it can remain or move off by runoff or leaching to surface or ground waters producing water bodies contamination (D'Ascenzo et al., 1998; Safarpour et al., 2004; Boithias et al., 2011; Hermosín et al., 2013; Belenguer et al., 2014; De Gaetano et al., 2016). In addition, pesticides are considered dangerous and harmful to human and ecosystem health because of their toxicity and carcinogenicity even at low concentrations (Damalas and Eleftherohorinos, 2011; Belenguer et al., 2014; Morris et al., 2016), being crucial to develop application strategies to prevent or minimize their transport and presence in water. One possible strategy is to support the pesticide on soil-compatible nanoadsorbents or nanocarriers, as controlled release formulations that minimize the pesticide transport losses responsible for water contamination (Lagaly, 2001; Nennemann et al., 2001; Rytwo and Tropp, 2001; Ulibarri and Hermosín, 2001; Celis et al., 2002; Carrizosa et al., 2004; Dupin et al., 2004; Cardoso et al., 2006; Hermosín et al., 2006; Radian and Mishael, 2008; Bruna et al., 2009; Chevillard et al., 2012; Kah et al., 2013; Pérez-de-Luque and Hermosín, 2013; Cabrera et al., 2016; Nuruzzaman et al., 2016). The adsorbent would act as a smart delivery system that, once located in the appropriate place (soil, plant leaves, rhizosphere), could decrease pesticide losses and, at the same time, maintain or increase the efficacy by the improvement of the target precision or location. Those adsorbent-pesticide preparations are lastly being labelled as nanoformulations or nanopesticides (Kah et al., 2013; Pérez-de-Luque and Hermosín, 2013; Nuruzzaman et al.,

2016), but they need to be subjected to deep study to accomplish the regulatory normative that pesticides need to be authorized (Walker et al., 2018).

Anionic or acidic water-soluble pesticides are particularly dangerous to be disseminated in environmental compartments, because they are weakly adsorbed by the soil components and hence they easily reach the water bodies. Therefore, there is special interest to develop adsorbents for those compounds. Two soil-friendly carrier materials appropriate for acid and anionic pesticides are the natural cationic or organo-modified clays (Lagaly, 2001; Celis et al., 2002, 2012; Carrizosa et al., 2004; Hermosín et al., 2006; Radian and Mishael, 2008; Chevillard et al., 2012; Pérez-de-Luque and Hermosín, 2013; He et al., 2014; Cabrera et al., 2016; Nuruzzaman et al., 2016) and the magnesium/aluminum layered double hydroxides (Mg/Al LDH) or anionic clays (Ulibarri and Hermosin, 2001; Dupin et al., 2004; Cardoso et al., 2006; Forano et al., 2006; Bruna et al., 2009; Nuruzzaman et al., 2016), because they are based on naturally occurring soil materials and they have been shown to interact with acid and anionic organic species, which can be hosted in their interlayer spaces from where they can be slowly released (Pérez-de-Luque and Hermosín, 2013; Nuruzzaman et al., 2016).

Imazamox (Imz), 2-[(RS)-4-isopropyl-4-methyl-5-oxo-2-imidazolin-2-yl]-5-methoxymethylnicotinic acid (Fig. S1), is an imidazolinone systemic herbicide used either pre- or post-emergence for broad-leaved weed control in several crops such as legumes, maize or sunflower (Eizenberg et al., 2009; Walker et al., 2018). One of its main use is to control broomrape, a very severe weed which parasites the crops in the roots, living most the time in the subsoil and, once the attack is visible, it is often too late to be controlled (Cessna et al., 2012). Even more, once the crop roots begin to develop, they release signaling compounds that stimulate the broomrape seeds to germinate and parasite them (Pérez-de-Luque et al., 2010). For that very reason, it is very important to develop Imz

formulations that allow the active ingredient to remain in the subsoil, to avoid, as earlier as possible, the broomrape attack. Radian and Mishael (2008) reported controlled release formulations for imazapyr, also an imidazolinone herbicide, based on organo-polymeric cationic clay and, more recently, Cabrera et al. (2016) showed the ability of inorganic (Fe^{3+})- and biopolymer-smectites to act as supports for the smart delivery of Imz. In the present work, we address two different supporting materials, five different methods of preparation, and higher loadings of herbicide in Imz nanoformulations. Although the Imz recommended field doses are very low, in fields where a continuous use is needed because of chronic soil infection (Xie et al., 2010), and in farm herbicide manipulation places, extensive imazamox leaching or runoff from the soil is possible (Aichele and Penner, 2005; Eizenberg et al., 2009). In fact, the presence of Imz in some environmental water samples has been reported (D'Ascenzo et al., 1998; Walker et al., 2018).

The objective of this study was to assess and compare the potential use of a commercial organoclay, Cloisite 10A (Clo10A), and a lab-synthesized layered double hydroxide (LDH) as very different soil-compatible matrices for obtaining controlled release Imz nanoformulations. Those nanoformulations should reduce the free herbicide concentration in soil solution, decreasing the herbicide losses by leaching or runoff and hence its potential risk of reaching ground or surface waters, while maintaining the efficacy. Diverse methods of clay-Imz complex preparation were assayed and their herbicide release patterns measured and related with their structure and interaction mechanisms.

2. Materials and methods

2.1. Reagents and soil

All inorganic reagents ($Mg(NO_3)_2 \cdot 6H_2O$, $Al(NO_3)_3 \cdot 9H_2O$, NaOH and Na_2CO_3) used to prepare the diverse LDH compounds were of technical grade purchased from Sigma-

120 Aldrich (98-99%). Technical grade Imz (98%), supplied by DpQ (Seville, Spain), was
121 utilized in this study in its acidic form, which has a water solubility of 620 mg L^{-1} and pKa
122 values of 3.2, 8.2 and 10.2. The commercial organoclay Cloisite 10A (Clo10A) used to
123 prepare the cationic clay nanoformulations is a modified quaternary alkylammonium
124 montmorillonite, from BYK Additives & Instruments, which was provided by Comindex
125 SL (Spain). The soil used in the experiments was a Rendisol from the experimental farm of
126 the University of Mostaganem (Algeria). The soil was sampled (0-20 cm), air-dried, and
127 sieved (2 mm) prior to use. Relevant physicochemical characteristics of the soil and X-ray
128 diffraction patterns of its clay (< 2 μm) fraction are provided in Table S1 and Fig. S2 of the
129 Supplementary material, respectively.
130
131 *2.2. Preparation of the Imazamox nanoformulations*
132 The Imz nanoformulations with LDH were prepared by two ways: (i) direct synthesis
133 (DS), using the conventional coprecipitation method described by Cardoso et al. (2006)
134 and ii) regeneration (RE) of calcined LDH (500ºC, LDH500), in aqueous solution
135 containing herbicide (Ulibarri and Hermosin, 2001; Pavlovic et al., 2005; Cardoso et al.,
136 2006). The LDH used was previously synthesized following the method of Reichle (1986).
137 To obtain the Imz-LDH nanoformulation by DS, a solution containing 0.02 mol of
138 $Mg(NO_3)_2$ and 0.01 mol of $Al(NO_3)_3$ was added dropwise under nitrogen atmosphere with
139 vigorous stirring to a solution containing 0.075 mol of NaOH and 0.03 mol of Imz. The
140 resulting gel was aged at 65ºC for 24 h, separated by centrifugation, washed with
141 decarbonated water, and dried at 50ºC to obtain the product denoted Imz-LDH DS. To
142 prepare the nanoformulation by RE, 0.5 g of the calcined LDH (LDH500) was added to a
143 solution (500 mL) containing 6 mmol of Imz dissolved in deionized water under nitrogen
144 flux. The dispersion was kept under vigorous stirring for 16 h, and then the mixture was

centrifuged and washed with decarbonated water and finally dried at 50°C to obtain the final product denoted Imz-LDH RE.

The Imz-Clo10A complexes (20% w/w) were prepared, according to Carrizosa et al. (2004), by three ways: (i) ground mix (GM), by adding 400 mg of Clo10A and 100 mg of Imz in an agate mortar and thoroughly hand-grinding for 10 min; (ii) weak complex (WC), by weighing the same amounts as above in a Pyrex screw cap bottle, 2 mL of methanol were added and shaken by vibration for 1 min, then the bottle was opened and allowed to dry until complete evaporation of the methanol; after that the complex was gently hand-ground in an agate mortar; (iii) strong complex (SC), prepared in the same way as the WC, but shaking the solid-methanol dispersion in a rotary shaker for an extended period of 24 h.

2.3. Characterization of the Imazamox-clay nanoherbicides

The metals contents of LDH were measured by ICP, after acid dissolution. CHN element chemical analyses were conducted using a Perkin-Elmer, model 1106, element analyzer. Powder X-ray diffraction patterns were recorded on a Siemens D-5000 diffractometer (Stuttgart, Germany) with CuKα radiation from 2 to 70° and at a 2Θ rate of 1.2° min^{-1}. The FTIR spectra were recorded on a Jasco FR/IR 6300 spectrometer after mixing and grinding the corresponding powder sample (2 mg) with KBr (200 mg) and pressing into a disc. The particle-size distribution and Z-potential was measured using a Malvern Master Z-Sizer. The samples were also characterized by scanning electron microscopy (SEM) using a JEOL 6460LV scanning electron microscope. The Imz content in the LDH-nanoformulations was measured by dissolving 2 mg of the corresponding complex in 2 mL of HCl (35%). Next, the volume was adjusted to 25 mL with an 80:20 diluted H_3PO_4:acetonitrile solution and then filtered and quantified by HPLC (Table S2). The study of the stability of the Imz-LDH complexes was also performed by monitoring

the Imz content of the complex over time, as described above.

2.4. Batch release study

The release of the active ingredient (Imz) from the diverse nanoformulations and also from the technical grade product was monitored using a batch method. Triplicate samples of 3 mg of technical Imz or the corresponding amount of the nanoformulations were mixed with 250 mL of distilled water in 500 mL amber glass bottles closed with screw caps. The bottles were hand-shaken for 1 min at selected times (10 min to 144 h) for sampling with a syringe, 2.5 mL-aliquots, which were filtered and analyzed by HPLC for Imz concentration. The data were fitted to a modified Fickian model equation: $M_t/M_z = k\ t^n + c$ (Ritger and Peppas, 1987; Cardoso et al., 2006), where M_t/M_z is the percentage released at time t, k is a rate constant associated to the formulation, and c is the amount instantaneously released.

2.5. Soil dissipation study

The soil persistence or dissipation study was carried out by incubation of soil (300 g), air-dried and sieved by 2 mm mesh, with a moisture content equivalent to 40%. The soil was placed in duplicate glass bottles and treated with a solution of commercial Imz (Pulsar 40, 4% active ingredient, a.i. w/v) or with the different Imz complexes to give a final concentration of 70 mg kg^{-1}. After various incubation times, duplicate 5 g of soil samples were removed from the bottles and extracted with 10 mL of mobile phase (80% diluted H_3PO_4:20% acetonitrile). The soil samples were centrifuged, and the supernatants were filtered (0.45 μm) prior to analysis of Imz residues by HPLC.

195 *2.6. Soil column leaching*

196 The study of the soil movement of Imz was performed using triplicate glass columns
197 (20 cm length × 3 cm internal diameter). The bottom of the columns was filled with glass
198 wool and 10 g of sea sand to prevent soil losses by leaching of fine particles. Next, the
199 columns were hand-packed with 180 g of soil, and 10 g of sea sand was placed on the top
200 to minimize the disturbance of the soil surface and to allow even distribution of water. A
201 volume of 100 mL of water was applied to saturate the columns and avoid variations in the
202 soil water content between them. After drainage, an aqueous solution of technical Imz,
203 Pulsar 40, or the solid nanoherbicide was carefully applied at 7000 g a.i. ha^{-1}, an amount
204 higher than the mean field application rate, but needed to facilitate detection by our
205 available HPLC technique (UV-diode array detector) for so many replicates. In the case of
206 the solid nanoherbicide formulations, they were suspended in the same water volume as
207 that used for the application of technical Imz and Pulsar 40, and then carefully applied on
208 the top of the corresponding columns. Daily, 15 mL of distilled water was applied to the
209 soil columns and the leachates were collected, filtered, and analyzed by HPLC.

210

211 *2.7. Bioassay*

212 The herbicidal activity of the different formulations prepared was tested with *Brassica*
213 *nigra* and compared with that of the commercial formulation of Imz (Pulsar 40) and with
214 controls without herbicide treatment. Triplicate pots (31 cm^2 surface area) were filled with
215 120 g of soil, saturated with water, and allowed to drain for 24 h. Then, twelve seeds of
216 *Brassica nigra* were gently distributed on the surface of each pot, and a small quantity of
217 soil was added to cover them. This plant species had previously been checked as very
218 sensible for Imz bioassay efficacy. Commercial Imz (Pulsar 40), Imz-LDH, and Imz-
219 Clo10A formulations were applied at a field rate of 70 g ha^{-1}. The pots were watered daily

with tap water. The biomass of the aerial and root part of the plants was weighed 2 weeks after the seeds were planted.

2.8. Data analysis

For duplicate or triplicate release, leaching, and bioassay experiments, statistical analysis was performed using the SPSS for Windows v.15 program. In the case of the bioassay, one way ANOVA test was used and all pairwise multiple comparisons were carried out using the HSD Tukey's test. Differences between treatments were considered statistically significant at $P < 0.05$.

3. Results and discussion

3.1. Physicochemical characterization

3.1.1. Initial materials

The physicochemical properties of Clo10A and synthesized LDH are summarized in Table 1. The results showed that the atomic ratio Mg/Al of LDH is 2.20 and the C/Al ratio is 0.51. The empirical formula of LDH deduced from the chemical analysis is $Mg_{0.69}Al_{0.31}(OH)_2(CO_3)_{0.16}{\cdot}mH_2O$ (m ~ 0.2, calculated by difference), which would correspond to an anion exchange capacity (AEC) for the material of 380 cmol(-) kg^{-1}. The original LDH-CO_3 synthesized sample displayed the characteristic XRD reflections of these lamellar compounds (Fig. 1) (Safarpour et al., 2004). The zeta potential is positive and similar to that reported by other authors (Xu et al., 2008), as due to the positive layer charge in LDH not being fully balanced on the external surfaces by carbonate or other anions in solution at the electric double layer.

The commercial sample Clo10A, due to its excess in organic cation saturation (>200%), is highly hydrophobic and its water dispersion resulted not homogeneous. Consequently,

245 the average particle size and Z-potential could not be consistently measured. The XRD of
246 Clo10A showed a basal spacing value of 19.13 Å (Fig. 2), corresponding to a
247 pseudotrimolecular conformation of the alkylammonium cations in the interlayer (Xu et
248 al., 1997; Nigmatullin et al., 2008). The XRD of technical Imz displayed a very well
249 defined reflection at 12.53 Å (not shown).
250
251 *3.1.2. Imazamox-clay complexes*
252 *3.1.2.1. X-ray diffraction.* The X-ray diffractograms of the Imz-LDH nanoherbicides
253 obtained by direct synthesis (DS) and by reconstruction (RE) are shown in Fig. 1. The
254 diffractograms of Imz-LDH DS and RE showed the successful intercalation of Imz by
255 direct synthesis (8.70 Å, Imz-LDH DS) and regeneration (21.44 Å, Imz-LDH RE), where
256 the position of the basal reflections shifted to a higher d_{003} value compared to the water
257 reconstructed LDH500 (LDH-R, 7.59 Å), indicating the expansion in the interlayer
258 distance (Hermosín et al., 2006). The different values for the (003) reflections obtained for
259 DS and RE suggested different interlayering in the complexes. The larger basal spacing
260 value for Imz-LDH RE indicated that larger amount of Imz anions was hosted in the RE
261 complex than in the DS complex, as was confirmed by HPLC analysis given in Table 2.
262 However, even assuming that all Imz was in the anionic form, the Imz content in Imz-LDH
263 DS represented only around 14% of the AEC of the original LDH, and 30% in the case of
264 Imz-LDH RE. Hence, other anions such as CO_3^{2-}, OH^- and NO_3^- would share the
265 interlayers with Imz anions. Fig.1 also shows an increase of the structural disorder for Imz-
266 LDH RE, as suggested by the overlapping and broadening of the (110) (1.52 Å) and (113)
267 (1.49 Å) reflections, whereas for Imz-LDH DS the same (110) and (113) reflections are
268 well defined, showing good crystallization, probably facilitated by the hydrothermal

treatment and also by the low Imz content (Ulibarri and Hermosín, 2001; Cardoso et al., 2006). No Imz as pure separate crystals was detected.

The large Imz content and the large size of this anion forces it to conform an organic bilayer in Imz-LDH RE with a steeply position in the interlayer space leading to a basal spacing value of 21.44 Å, whereas in Imz-LDH DS, Imz anions must conform a monolayer in flat position rendering a broad reflection at 8.70 Å, in both cases with a mixed distribution of Imz^-, CO_3^{2-}, OH^-, and in DS, also NO_3^- anions. These arrangements are schematized in Fig. 1.

The X-ray diffractograms of the three types of complexes or nanoformulations with Clo10A (Fig. 2) show important differences. The Imz-Clo10A GM develops as a mix of the Clo10A, with its unchanged basal reflection at 19.13 Å, besides a very well defined reflection of pure Imz at 12.77 Å. In contrast, the Imz-Clo10A WC and SC both show a clear increase of their basal reflection to 22.68 Å, indicating that some Imz molecules or anions have been intercalated in the interlayer space of Clo10A. However, some free recrystallized Imz is denoted also by its 12.77 Å reflection. Similar interlayer complexes have been reported earlier for other acid herbicides such as 2,4-D, bentazone and dicamba (Bruna et al., 2009; Carrizosa et al., 2004).

3.1.2.2. FT-IR spectroscopy. The presence of Imz in the diverse complexes was verified by comparison of the FT-IR spectra of the corresponding initial matrix (LDH-CO_3 or Clo10A), pure Imz, and the nanoherbicides (Fig. 3). Fig. 3A and 3B display the Imz spectrum showing, as most relevant bands, those at 3220 cm^{-1}, assigned to NH stretching of the amide group of the lactam ring, and at 1745 cm^{-1}, assigned to the carbonyl bond of the carboxylic acid group in the imidazol and pyridine rings, and bands from 1696 to 1650 cm^{-1} and from 1465 to 1369 cm^{-1} corresponding to ring breathing modes of both heterocycles, accordingly with their chemical structure (Fig. S1). The spectra

294 corresponding to Imz-LDH complexes (DS and RE, Fig. 3A) show diverse bands
295 corresponding to Imz in the range 1740-500 cm^{-1}, which are better developed in the case of
296 RE complex than for DS. The most noticeable fact in Imz-LDH RE is the appearance of a
297 new band at 1575 cm^{-1}, which should correspond to the anionic form (carboxylate) of Imz,
298 accompanied by a decrease in the diverse bands corresponding to the acid form (1745,
299 1696 and 1650 cm^{-1}). The 1575 cm^{-1} band is not well defined in the Imz-LDH DS
300 complex, which also reveals the presence of nitrate in the interlayer by the very strong and
301 sharp band at 1383 cm^{-1} (Carja et al., 2002; Halajnia et al., 2013). The lower loading of
302 Imz anion in the interlayer of Imz-LDH DS is confirmed by the low, almost imperceptible,
303 decrease of the broad 3420 cm^{-1} band of OH stretching of interlayer water with respect to
304 that observed for RE. The presence of a band at 1379 cm^{-1} in Imz-LDH RE shows the
305 coexistence of interlayer CO_3^{2-}.

306 The FT-IR spectra of Imz-Clo10A GM, WC and SC complexes, shown in Fig. 3B,
307 reveal the presence of Imz bands at 3220, 1750, 1684, 1656 and 1469 cm^{-1}, beside the
308 bands corresponding to the original Clo10A. In this case, no new bands corresponding to
309 Imz anion were identified, and hence it is probable that most of the herbicide remained
310 associated as neutral molecules H-bonded to the interlayer or external alkylammonium
311 ions (Hermosín and Cornejo, 1993).

312 *3.1.2.3. Size, morphology and Z-potential of particles.* The average particle size (APS,
313 Table 2) of the Imz-LDH RE and Imz-LDH DS complexes decreased to 306 and 225 nm,
314 respectively, compared to the particle size of the original LDH (429 nm). This decrease in
315 particle size probably occurred because the crystal tension produced by the intercalation of
316 the large organic anion imazamox, either by direct synthesis or reconstruction, produced
317 fragmentation, rendering smaller particles. These smaller particle sizes agree with the
318 crystallinity loss detected by XRD. The Zeta potential values (Table 2) show that there is

not a large association of organic anions at external surfaces, but just the contrary; less external anion seems to be associated in the Imz-LDH complexes than those in inorganic initial LDH material, since the surface Z potential increased (Table 1 and 2). Thus, the Imz at the external LDH surfaces will be as neutral acid molecules. This fact also confirms the success of the process of intercalation with a large amount of Imz lodged in the interlayer space of Imz-LDH.

The scanning electron micrographs (Fig. 4) show that the LDH-CO_3 is well-formed with its typical hexagonal morphology and regular sized microcrystals. The morphology of both nanoformulations was fairly different from that of LDH, with non-uniform irregular agglomerates of compacted and non-porous plate-like structure (Costa et al., 2008). In the case of the complexes Imz-LDH RE and DS, they showed slightly larger compaction as compared with the original LDH, as a result of its Imz content which favors lipophilic attraction between the particles rendering aggregation, in agreement with APS measurements (Table 2).

The SEM images showed that Clo10A (Fig. 4b1), due to its alkylammonium excess, formed aggregates where the easily visible layered package crystals are joint together by lipophilic forces in irregular stacking forms. The Imz-Clo10A GM shows forms very similar to the clay alone, but with larger agglomeration (Fig. S3a). The 24 h methanol-treated Clo10A (blank for the Imz-Clo10A SC) (Fig. S3b) showed larger ordered aggregation in flat, big particles with opened structure, with some small rolled-up forms, probably because of alkylammonium-methanol interactions which change or homogenize the conformation of the interlayer (Lagaly and Dékany, 2005), facilitating a well-oriented sedimentation. However, the Imz-Clo10A WC and SC showed some noticeable differences. The WC sample (Fig. 4b2) displays a large aggregation effect but as conglomerated disordered crystals, with some stacking order inside, whereas in SC sample

(Fig. 4b3) medium-large aggregates of rolled-up structure are developed and formed by compacted particles. This rolled-up aggregation displayed for SC should be due to the presence of Imz, because, after 24 h of contact with methanol, Clo10A alone displays only small structure like that, besides some ordered layered stacking in open structures (Fig. S3b). Those interactions must affect also the interlayer/external distribution of the herbicide, but no to a great extent, because both WC and SC rendered the same basal spacing value (Fig. 2). The SEM images, besides XRD results, suggest that Imz molecules in Imz-Clo10A complexes distribute at different rates both outside at interparticle (GM, WC and SC) surfaces and at inner or interlayer surfaces (WC and SC). Although XRD showed diverse proportion of crystallized Imz (GM > WC ≈ SC), this was not appreciated by SEM.

3.2. Release of imazamox in water

The herbicide release profiles in water from the (free) technical product (technical Imz) and the nanoformulations are shown in Fig. 5. The Imz-Clo10A GM formulation released or solubilized almost all its herbicide content instantaneously, thus showing an immediate release (93%) very similar to that of technical Imz (98.5%), but with a very short initial delay of 10 h. In contrast, the release percentage profiles of Imz-LDH RE, DS and Imz-Clo10A WC and SC displayed a true slow release pattern beginning with different immediate release amounts, always higher than 50%, which increased stepwise to a total amount higher than 70% (Fig. 5). The amount immediately released corresponds to the active ingredient outside the clay particles, which is immediately dissolved, followed by the diffusion and detachment of the interlayer Imz molecules or anions. The lower release for Imz-LDH DS complex, as compared with that for RE, could be related with its lower content of Imz, whose molecules remain tightly bonded in a thinner interlayer, according

to the X-ray diffractograms and to the conformation given in Fig. 1. That thinner interlayer and the closeness of layer-Imz-layer prevent the detachment of the Imz anions to be substituted by carbonate coming from atmospheric CO_2 or hydroxyl anions. The smaller particle size of this Imz-LDH DS complex (Table 2) did not appear to influence the release.

The slow release of Imz-Clo10A WC and SC for the first 24 h is justified by a resistance to desorption of Imz anion, because of the stronger interactions between the large amount of alkylammonium ions on the clay and Imz. This would agree with the interaction mechanism proposed above where the herbicide, as molecule or even as anion, would be adsorbed at the external surfaces by hydrogen bonds and also within the organoclay galleries, through stronger hydrophobic interactions with the alkyl moieties of the organic cations (Bruna et al., 2009; Chevillard et al., 2012). These results are consistent with those of XRD. Contrary to what expected, the total amount of Imz released from Imz-Clo10A WC (82.5%) was lower than from Imz-Clo10A SC (92.8%), so that the cloisite-imazamox interaction time did not directly determine the release profile of the resulting complex. The presence of alcohol may have caused certain changes in the alkylammonium conformation in the interlayer and even some displacement of the alkylammonium excess to the external surface (Lagaly and Dékany, 2005) affecting Imz-Clo10A interactions; hence, larger interaction times could, by this way, weaken the Imz-alkylammoniun H-bonds, facilitating the herbicide release in SC complex. In fact, those commented differences should be due to interactions at molecular level, because the SEM observations do not explain the different release behavior of WC and SC. According to Fig. 5, the performance of the complexes as slow-release systems decreased in the order: Imz-LDH RE > Imz-Clo10A SC > Imz-Clo10A WC > Imz-Clo10A GM > Imz-LDH DS. The fitting of the release data to the modified Fickian kinetic equation rendered the parameters

summarized and discussed in the supplementary material (Table S3), confirming the above discussion.

3.3. Soil environmental behavior

3.3.1. Stability and soil dissipation of Imazamox-clay complexes

Since the soil degradation of Imz has been reported to increase at pH 7 compared to lower pH levels (Aichele and Penner, 2005) and given the basic environment on the interlayer surface of LDH (Reichle, 1986; Xu et al. 2008; Debecker et al., 2009), the stability of both Imz-LDH complexes prepared was monitored. The results are shown in Fig. S4a and revealed that the amount of the active ingredient Imz remained practically constant along 60 days in both complexes. This was confirmed by recording the X-ray diffractograms, which rendered the same basal spacing values as the freshly prepared Imz-LDH complexes. Thus, the interlayer position of Imz anions did not affect the stability of the herbicide.

Fig. S4b displays the soil dissipation curves of all the Imz complexes (Imz-LDH and Imz-Clo10A) besides those corresponding to the technical product and commercial formulation. The curves show no significant differences in persistence among all forms of the soil-applied herbicide. This result is noteworthy because it shows that insertion or support of the herbicide in the complexes does not alter the Imz persistence in soil as compared with (free) technical or commercial formulation products.

3.3.2. Column leaching study

The breakthrough curves (BTCs) of Imz applied to soil columns as free technical compound (technical Imz), as commercial form (Pulsar 40), and as the diverse Imz-clay complexes are shown in Fig. 6. For the relative BTCs, all complexes have similar leaching

profiles with the maximum concentration appearing close to 75 mL, except for the Imz-LDH DS complex, where the position of the maximum concentration peak is located close the column pore volume (56 mL). Technical and commercial (Pulsar 40) Imz gave a maximum concentration of 18 and 16 mg L^{-1}, respectively, which decreased to 13, 11 and 12.5 mg L^{-1} for Imz-Clo10A GM, WC and SC and to 14.5 and 14 mg L^{-1} for Imz-LDH RE and Imz-LDH DS, respectively. Fig. 6 shows that the total amount of Imz leached from the technical and commercial forms reached 90-100%, whereas that from the complexes ranged from 67 to 77%, in close agreement with the Imz release profiles. The total amount of Imz leached from the complexes followed the order: Imz-Clo10A WC < Imz-Clo10A SC < Imz-LDH RE < Imz-LDH DS < Imz-Clo10A GM. Thus, the prepared complexes showed a very wide range of herbicide soil leaching decrease. It is noticeable that the soil leaching profiles of the complexes are more similar among them than the water release profiles, showing all of them appropriate behavior. In fact, the role of the soil is also important.

Negligible residual Imz was detected after extraction of the soil columns at the end of the leaching experiment. Therefore, the difference between the amount of Imz added and that leached out from the soil columns can be attributed to soil degradation, besides some irreversible binding of the Imz to organoclay or LDH or even soil particles.

3.4. Efficacy bioassay

The herbicidal activity of the nanoherbicides prepared was compared with that of the commercial formulation (Pulsar 40) of Imz. Fig. 7 shows the mass of the aerial and root parts of *Brassica nigra* at the end of the bioassay. The decrease observed in the aerial and root biomasses for the Imz-clay complexes treatments with respect to the control were similar to that shown by the commercial formulation treatment; even the Imz-Clo10A

complexes seemed to improve the efficacy as compared with commercial Pulsar 40. These results indicated that all nanoherbicide complexes applied pre-emergence were as effective as the commercial formulated (Pulsar 40) herbicide in preventing *Brassica nigra* growth.

4. Conclusion

LDH and organic Cloisite 10A are shown to be good host materials to obtain imazamox (Imz) nanoformulations for use in controlled release, smart delivery systems to minimize leaching losses and hence water contamination. Imz, as anion or as neutral molecules, is located partially in the interlayer of both types of nanoclays, and on the external surface, even crystallized separately in the case of the Imz-Clo10A complex, depending of the support and preparation mode. The Imz-LDH and Imz-Clo10A complexes resulted structurally different, but they displayed similar behavior in water release and soil leaching, showing a diverse degree of immediate Imz availability followed by a slower and prolonged release. The main environmental advantage of applying the nanoformulations is the decrease in the maximum Imz concentration peak of the soil leachates, which decreases between 10 and 35% as compared with technical and commercial products while maintaining efficacy. Since Imz is a herbicide which acts at plant root level, formulations containing these Imz-clay nanoherbicides could be located in soil at 5-15 cm below the topsoil at the rhizosphere, where they will act as smart delivery systems closer to its target (*Broomrape seeds*), with the advantage of decreasing the herbicide concentration and release to surface and ground water from soil, thus minimizing the environmental impact of this herbicide to pollute waters.

Acknowledgments

This work was supported by Junta de Andalucía (Project P11-AGR-7400) and MINECO-CSIC (Project RECUPERA 2020), both co-financed by FEDER and FSE funds. Partial support by MINECO Projects AGL2014-51897-R and AGL2017-82141-R is also acknowledged. Prof Rachid Khatem thanks University of Mostaganem for Advanced Research Learning at Foreign Countries for supporting a stay at IRNAS-CSIC.

References

Aichele, T.M., Penner, D., 2005. Adsorption, desorption, and degradation of imidazolinones in soil. Weed Technol. 19, 154–159.

Belenguer, V., Martinez-Capel, F., Masiá, A., Picó, Y., 2014. Patterns of presence and concentration of pesticides in fish and waters of the Júcar River (Eastern Spain). J. Hazard. Mater. 265, 271–279.

Boithias, L., Sauvage, S., Taghavi, L., Merlina, G., Probst, J.L., Perez, J.M.S., 2011. Occurrence of metolachlor and trifluralin losses in the Save river agricultural catchment during floods. J. Hazard. Mater. 196, 210–219.

Bruna, F., Celis, R., Pavlovic, I., Barriga, C., Cornejo, J., Ulibarri, M.A., 2009. Layered double hydroxides as adsorbents and carriers of the herbicide (4-chloro-2-methylphenoxy)acetic acid (MCPA): Systems Mg–Al, Mg–Fe and Mg–Al–Fe. J. Hazard. Mater. 168, 1476–1481.

Cabrera, A., Celis, R., Hermosín, M.C., 2016. Imazamox-clay complexes with chitosan- and iron(III)-modified smectites and their use in nanoformulations. Pest Manag. Sci. 72, 1285–1294.

Cardoso, L.P., Celis, R., Cornejo, J., Valim, J.B., 2006. Layered double hydroxides as supports for the slow release of acid herbicides. J. Agric. Food Chem. 54, 5968–5975.

494 Carja, G., Nakamura, R., Niiyama, H., 2002. Copper and iron substituted hydrotalcites:
495 properties and catalyst precursors for methylamines synthesis. Appl. Catal. A Gen. 236,
496 91–102.
497 Carrizosa, M.J., Koskinen, W.C., Hermosín, M.C., 2004. Interactions of acidic herbicides
498 bentazon and dicamba with organoclays. Soil Sci. Soc. Am. J. 68, 1863-1866.
499 Celis, R., Adelino, M.A., Hermosín, M.C., Cornejo, J., 2012. Montmorillonite–chitosan
500 bionanocomposites as adsorbents of the herbicide clopyralid in aqueous solution and
501 soil/water suspensions. J. Hazard. Mater. 209–210, 67–76.
502 Celis, R., Hermosin, M.C., Cornejo, L., Carrizosa, M.J., Cornejo, J., 2002. Clay-herbicide
503 complexes to retard picloram leaching in soil. Int. J. Environ. Anal. Chem. 82, 503–517.
504 Cessna, A.J., Elliott, J.A., Bailey, J., 2012. Leaching of three imidazolinone herbicides
505 during sprinkler irrigation. J. Environ. Qual. 41, 882-892.
506 Chevillard, A., Angellier-Coussy, H., Guillard, V., Gontard, N., Gastaldi, E., 2012.
507 Controlling pesticide release via structuring agropolymer and nanoclays based
508 materials. J. Hazard. Mater. 205–206, 32–39.
509 Costa, F.R., Leuteritz, A., Wagenknecht, U., Jehnichen, D., Häußler, L., Heinrich, G.,
510 2008. Intercalation of Mg–Al layered double hydroxide by anionic surfactants:
511 Preparation and characterization. Appl. Clay Sci. 38, 153–164.
512 Damalas, C.A., Eleftherohorinos, I.G., 2011. Pesticide exposure, safety issues, and risk
513 assessment indicators. Int. J. Environ. Res. Public Health 8, 1402–1419.
514 D'Ascenzo, G., Gentili, A., Marchese, S., Perret, D., 1998. Development of a method
515 based on liquid chromatography-electrospray mass spectrometry for analyzing
516 imidazolinone herbicides in environmental water at part-per-trillion levels. J.
517 Chromatogr. A 800, 109–119.

518 Debecker, D.P., Gaigneaux, E.M., Busca, G., 2009. Exploring, tuning, and exploiting the
519 basicity of hydrotalcites for applications in heterogeneous catalysis. Chem. Eur. J. 15,
520 3920-3935.
521 De Gaetano, Y. Hubert, J., Mohamadou, A., Boudesocque, S., Plantier-Royon, R., Renault,
522 J.H., Dupont, L., 2016. Removal of pesticides from wastewater by ion pair Centrifugal
523 Partition Extraction using betaine-derived ionic liquids as extractants. Chem. Eng. J.
524 285, 596–604.
525 Dupin, J.-C., Martinez, H., Guimon, C., Dumitriu, E., Fechete, I., 2004. Intercalation
526 compounds of Mg–Al layered double hydroxides with dichlophenac: different methods
527 of preparation and physico-chemical characterization. Appl. Clay Sci. 27, 95–106.
528 Eizenberg, H., Hershenhorn, J., Ephrath, J.E., 2009. Factors affecting the efficacy of
529 *Orobanchecumana* chemical control in sunflower. Weed Res. 49, 308–315.
530 Forano, C., Hibino, T., Leroux, F., Taviot-Guého, C., 2006. Layered double hydroxides.
531 In: Bergaya, F., Theng, B.K.G., Lagaly, G. (Eds) Handbook of Clay Science. Elsevier,
532 Developments in Clay Science, Volume 1, Amsterdam, pp. 1021-1095.
533 Halajnia, A., Oustan, S., Najafi, N., Khataee, A.R., Lakzian, A., 2013. Adsorption–
534 desorption characteristics of nitrate, phosphate and sulfate on Mg–Al layered double
535 hydroxide. Appl. Clay Sci. 80–81, 305–312.
536 He, H., Ma, L., Zhu, J., Frost, R.L., Theng, B.K.G., Bergaya, F., 2014. Synthesis of
537 organoclays: A critical review and some unresolved issues. Appl. Clay Sci. 100, 22-28.
538 Hermosín, M.C., Cornejo, J., 1993. Binding mechanism of 2,4-Dichlorophenoxyacetic acid
539 by organo-clays. J. Environ. Qual. 22, 325-331.
540 Hermosin, M.C., Calderón, M.J., Real, M., Cornejo, J., 2013. Impact of herbicides used in
541 olive groves on waters of the Guadalquivir river basin (southern Spain). Agric. Ecosyst.
542 Environ. 164, 229–243.

Hermosín, M.C., Celis, R., Facenda, G., Carrizosa, M.J., Ortega-Calvo, J.J., Cornejo J., 2006. Bioavailability of the herbicide 2,4-D formulated with organoclays. Soil Biol. Biochem. 38, 2117–2124.

Kah, M., Beulke, S., Tiede, K., Hofmann, T., 2013. Nanopesticides: State of knowledge, environmental fate, and exposure modeling. Crit. Rev. Environ. Sci. Technol. 43, 1823–1867.

Lagaly, G., 2001. Pesticide-clay interactions and formulations. Appl. Clay Sci. 18, 205-209.

Lagaly, G., Dékany, I., 2005. Adsorption on hydrophobized surfaces: Clusters and self-organization. Adv. Colloid Interface Sci. 114–115, 189–204.

Morris, A., Murrell, E.G., Klein, T., Noden, B.H., 2016. Effect of two commercial herbicides on life history traits of a human disease vector, Aedesaegypti, in the laboratory setting. Ecotoxicology 25, 863–870.

Nennemann, A., Mishael, Y., Nir, S., Rubin, B., Polubesova, T., Bergaya, F., Van Damme, H., Lagaly, G., 2001. Clay-based formulations of metolachlor with reduced leaching. Appl. Clay Sci. 18, 265-275.

Nigmatullin, R., Gao, F., Konovalova, V., 2008. Polymer-layered silicate nanocomposites in the design of antimicrobial materials. J. Mater. Sci. 43, 5728–5733.

Nuruzzaman, M., Rahman, M.M., Liu, Y., Naidu, R., 2016. Nanoencapsulation, nano-guard for pesticides: A new window for safe application. J. Agric. Food Chem. 64, 1447–1483.

Pavlovic, I., Barriga, C., Hermosín, M.C., Cornejo, J., Ulibarri, M.A., 2005. Adsorption of acidic pesticides 2,4-D, Clopyralid and Picloram on calcined hydrotalcite. Appl. Clay Sci. 30, 125–133.

Pérez-de-Luque, A. Eizenberg, H., Grenz, J.H., Sillero, J.C., Avila, C., Sauerborn, J., Rubiales, D., 2010. Broomrape management in faba bean. Field Crop. Res. 115, 319–328.

Pérez-de-Luque, A., Hermosín, M.C., 2013. Nanotechnology and its use in agriculture, In: Bio-Nanotechnology, Blackwell Publishing Ltd., pp. 383-398.

Radian, A., Mishael, Y.G., 2008. Characterizing and designing polycation-clay nanocomposites as a basis for imazapyr controlled release formulations. Environ. Sci. Technol. 42, 1511–1516.

Reichle, W.T., 1986. Synthesis of anionic clay minerals (mixed metal hydroxides, hydrotalcite). Solid State Ionics 22, 135–141.

Ritger, P.L., Peppas, N.A., 1987. A simple equation for description of solute release II. Fickian and anomalous release from swellable devices. J. Control. Release 5, 37–42.

Rytwo, G., Tropp, D., 2001. Improved efficiency of a divalent herbicide in the presence of clay, by addition of monovalent organocations. Appl. Clay Sci. 18, 327–333.

Safarpour, H., Asiaie, R., Katz, S., 2004. Quantitative analysis of imazamox herbicide in environmental water samples by capillary electrophoresis electrospray ionization mass spectrometry. J. Chromatogr. A 1036, 217–222.

Ulibarri, M.A., Hermosin, M.C., 2001. Layered double hydroxides in water decontamination. In: Layered Double Hydroxides: Present and Future, Rives, V. (Ed), Nova Science Publishers, Inc. NY., pp. 251-284.

Walker, G.W., Kookana, R.S., Smith, N.E., Kah, M., Doolette, C.L., Reeves, P.T., Lovell, W., Anderson, D.J., Turney, T.W., Navarro, D.A., 2018. Ecological risk assessment of nano-enabled pesticides: A perspective on problem formulation. J. Agric. Food Chem. 66, 6480-6486.

591 Xie, X., Yoneyama, K., Yoneyama, K., 2010. The strigolactone story. Annu. Rev.
592 Phytopathol. 48, 93–117.
593 Xu, S., Sheng, G., Boyd, S.A., 1997. Use of organoclays in pollution abatement. Adv.
594 Agron. 59, 25–62.
595 Xu, Z.P., Jin, Y., Liu, S., Hao, Z.P., Lu, G.Q., 2008. Surface charging of layered double
596 hydroxides during dynamic interactions of anions at the interfaces. J. Colloid Interface
597 Sci. 326, 522–529.
598
599

Figure captions

Fig. 1. XRD patterns for original LDH (LDH-CO_3), calcined LDH (LDH-500ºC), LDH reconstructed from LDH500 (LDH-R), LDH-Imazamox DS (Imz-LDH DS) and LDH-Imazamox RE (Imz-LDH RE), and proposed interlayer arrangement of imazamox in Imz-LDH DS and Imz-LDH RE.

Fig. 2. XRD patterns of Clo10A, Imz-Clo10A GM, Imz-Clo10A SC and Imz-Clo10A WC (★ Imazamox crystallized diffraction).

Fig. 3. A) FT-IR spectra of Imazamox (a), Imz-LDH DS (b), Imz-LDH RE (c) and LDH-CO_3 (d); **B)** FT-IR spectra of Imz-Clo10A SC (a), Imz-Clo10A GM (b), Imz-Clo10A WC (c), Imazamox (d) and Clo10A (e).

Fig. 4. SEM micrographs of a1) LDH-CO_3, a2) Imz-LDH RE, a3) Imz-LDH DS and b1) Clo10A, b2) Imz-Clo10A WC, b3) Imz-Clo10A SC.

Fig. 5. Kinetics of the release of Imazamox into water.

Fig. 6. BTCs for Imazamox after application to soil columns as technical Imz, commercial herbicide (Pulsar 40) and nanoherbicides.

Fig. 7. Bioassay results.

Table 1

Physicochemical characteristics of the initial anionic (LDH) and cationic organic (Clo10A) clays used as supports for nanoformulations.

Sample	Elemental chemical analysis (%)					IEC[a]	Zeta P	APS[c]	d_{00l}	SSA_{BET}
	C	H	N	Mg	Al	(cmol kg^{-1})	(mV)	(nm)	(Å)	(m^2 g^{-1})
Clo10A	19.5	0.9	0.4	-	-	125[b]	-	-	19.13 (d_{001})	19.0
LDH	2.7	3.9	≤ 0.02	23.3	11.7	380	22	429	7.63 (d_{003})	91.8

[a]Ion Exchange Capacity: AEC for LDH and CEC for Clo10A.

[b]Nigmatullin et al. (2008).

[c]APS: Z-average particle size (diameter).

Table 2

Physicochemical characteristics of the different Imz-LDH complexes.

Sample	d_{003} (Å)	C (%)	H (%)	N (%)	Herbicide content[a]		APS[b]	Zeta P
					% mass	cmol kg^{-1} (%AEC)	(nm)	(mV)
Imz-LDH RE	21.44	21.8	4.8	4.9	35.1	115 (30%)	306	31.5
Imz-LDH DS	8.70	10.2	3.7	5.3	16.8	55 (14%)	225	33.7

[a]Measured by HPLC after sample dissolution.

[b]APS : Z-average particle size (diameter).

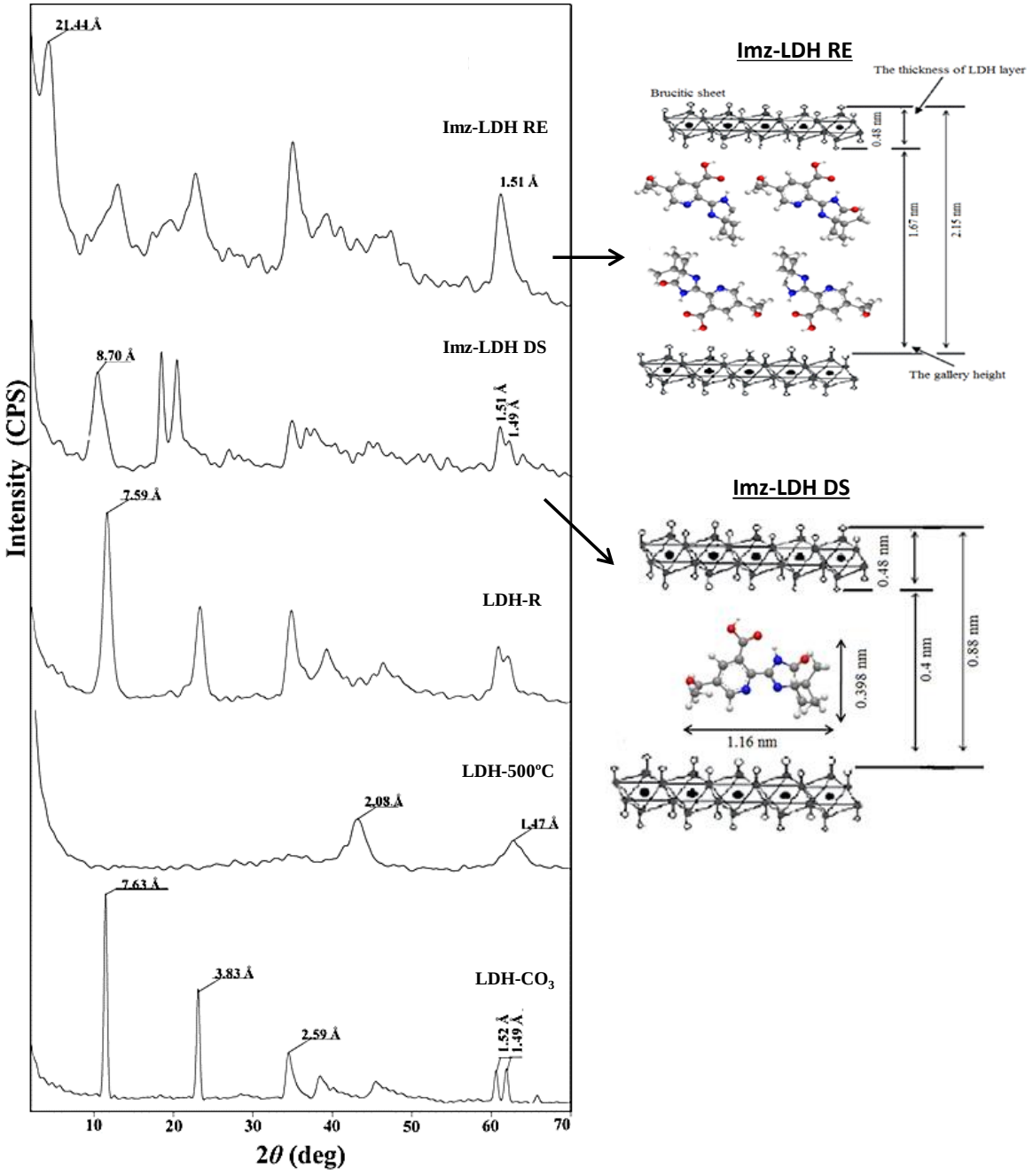

Fig. 1. XRD patterns for original LDH (LDH-CO_3), calcined LDH (LDH-500ºC), LDH reconstructed from LDH500 (LDH-R), LDH-Imazamox DS (Imz-LDH DS) and LDH-Imazamox RE (Imz-LDH RE), and proposed interlayer arrangement of imazamox in Imz-LDH DS and Imz-LDH RE.

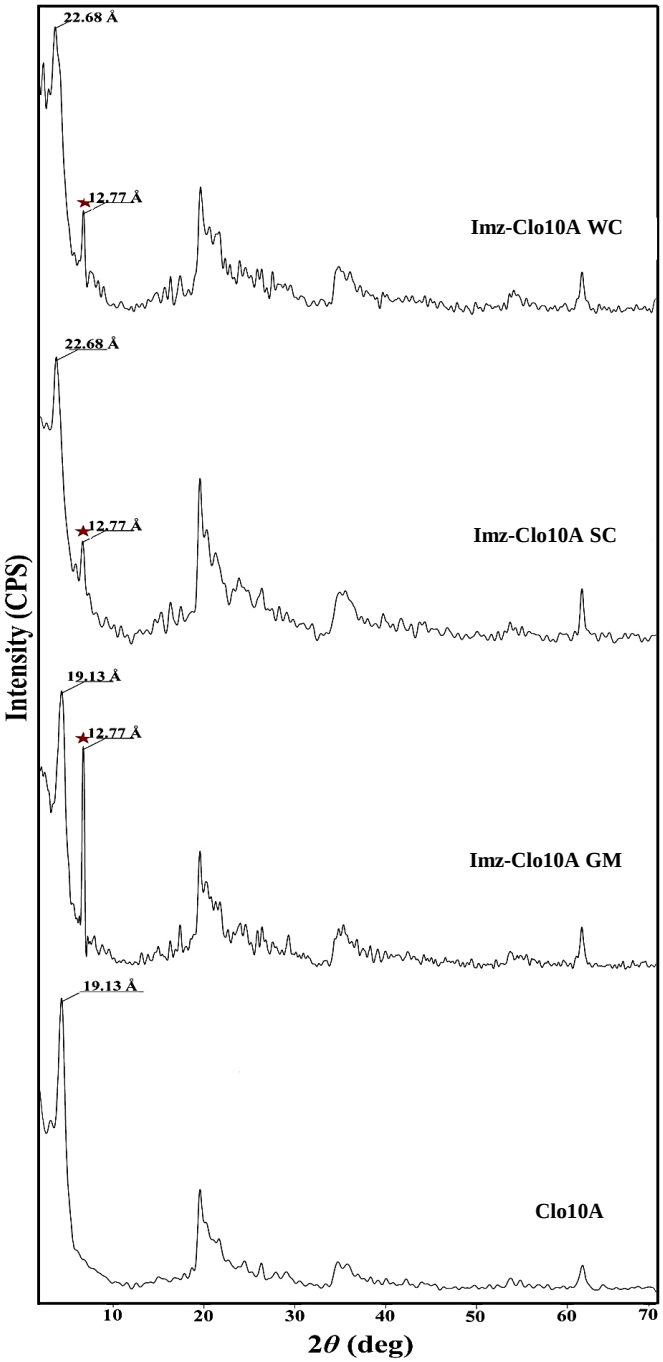

Fig. 2. XRD patterns of Clo10A, Imz-Clo10A GM, Imz-Clo10A SC and Imz-Clo10A WC (★ Imazamox crystallized diffraction).

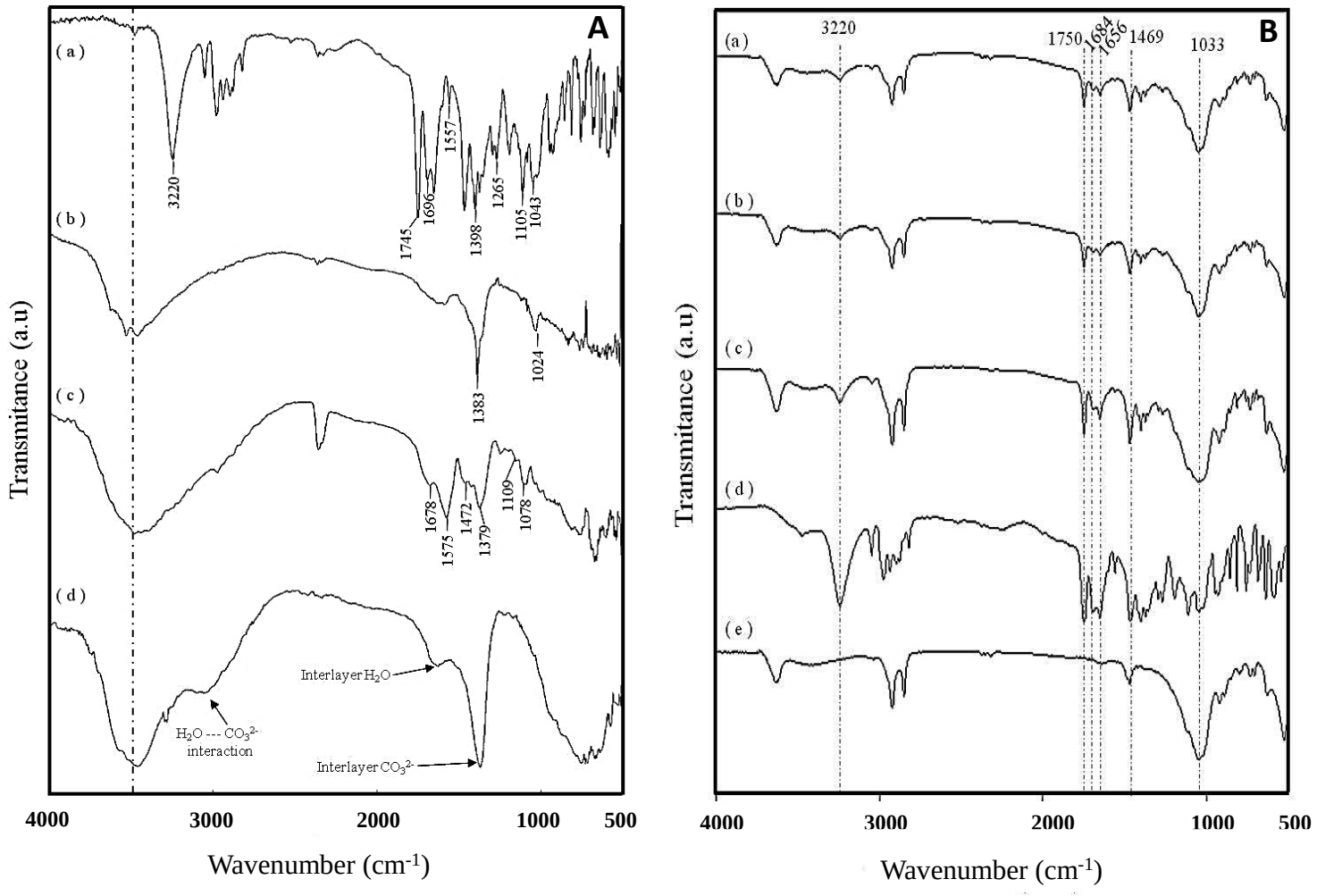

Fig. 3. A) FT-IR spectra of Imazamox (a), Imz-LDH DS (b), Imz-LDH RE (c) and LDH-CO_3 (d); **B)** FT-IR spectra of Imz-Clo10A SC (a), Imz-Clo10A GM (b), Imz-Clo10A WC (c), Imazamox (d) and Clo10A (e).

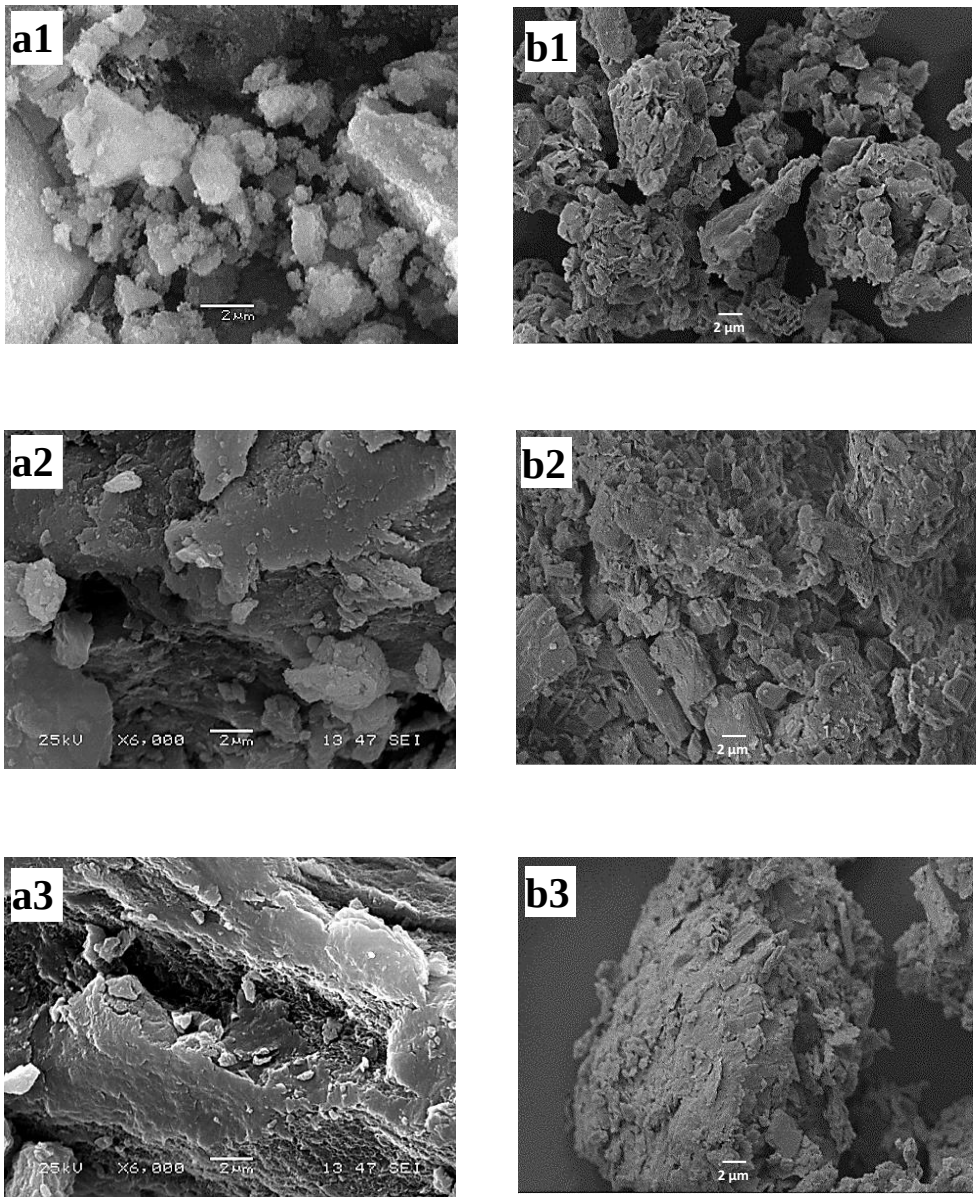

Fig. 4. SEM micrographs of a1) LDH-CO_3, a2) Imz-LDH RE, a3) Imz-LDH DS and b1) Clo10A, b2) Imz-Clo10A WC, b3) Imz-Clo10A SC.

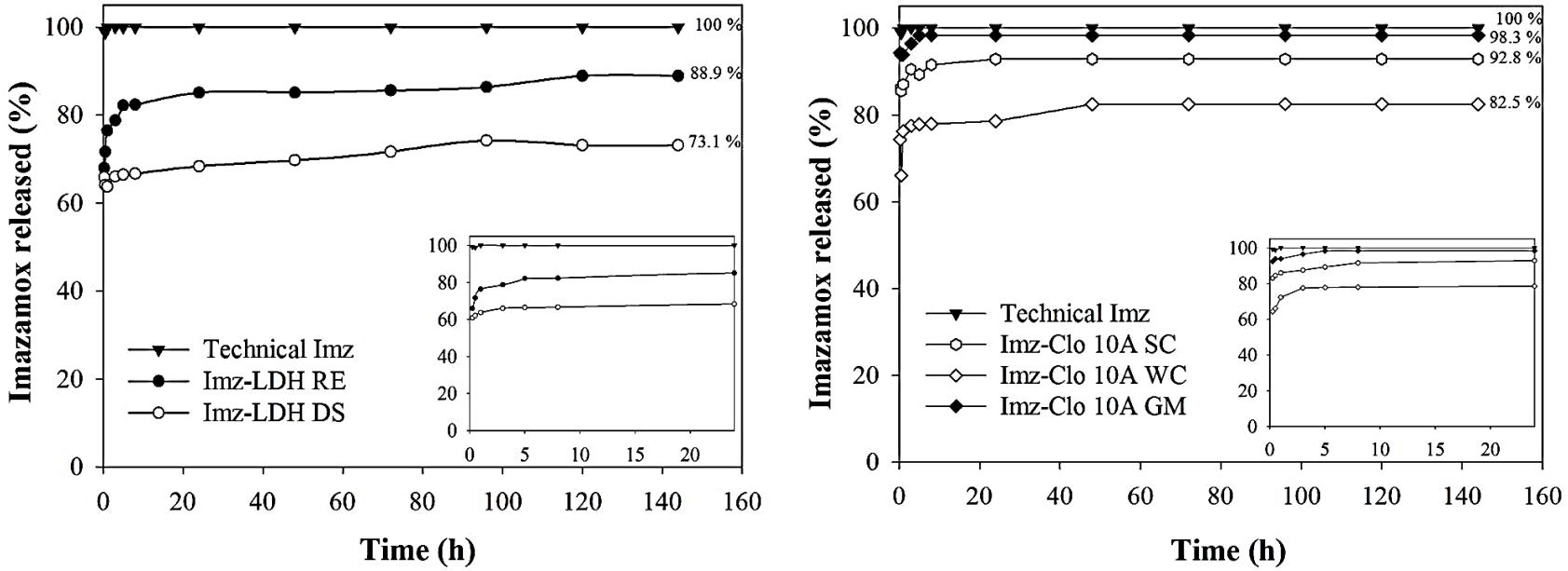

Fig. 5. Kinetics of the release of Imazamox into water.

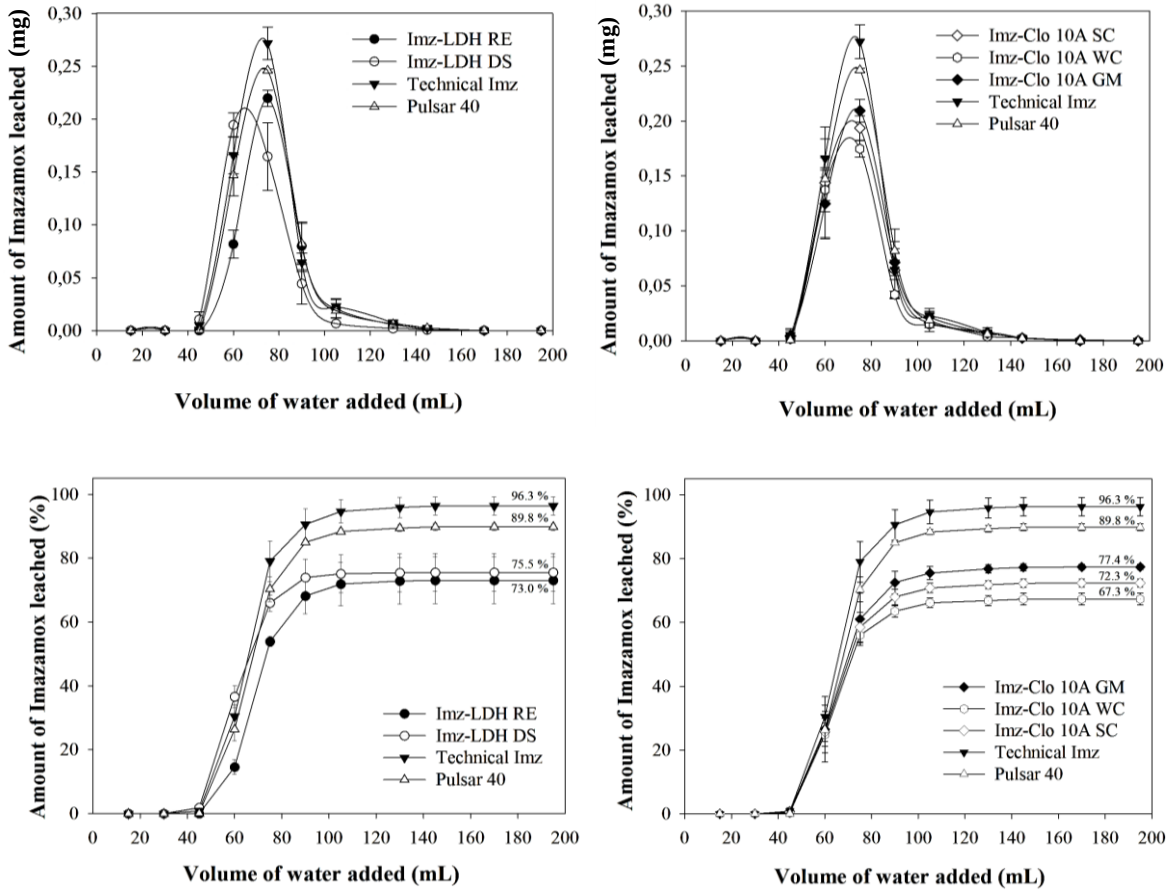

Fig. 6. BTCs for Imazamox after application to soil columns as technical Imz, commercial herbicide (Pulsar 40) and nanoherbicides.

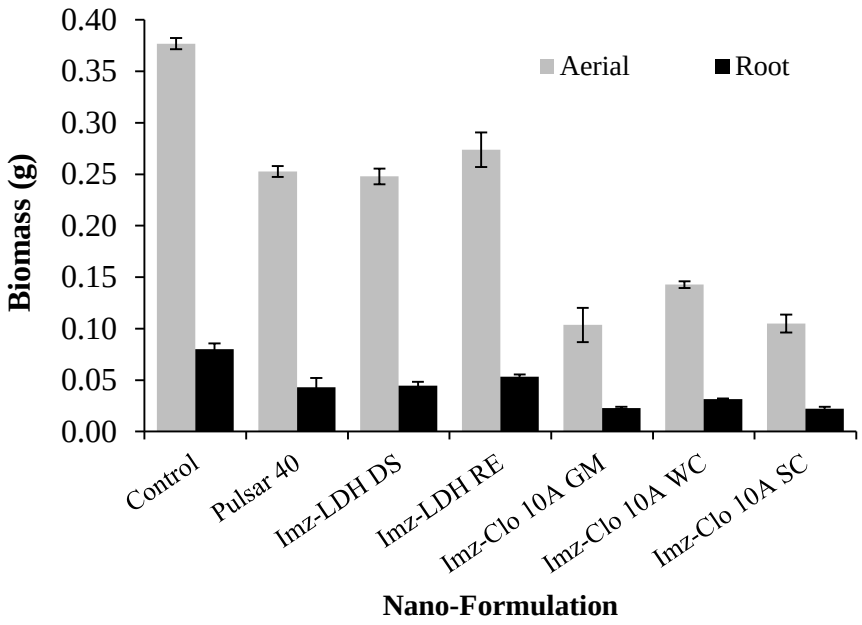

Fig. 7. Bioassay results.

Supplementary Information for

Cationic and anionic clay nanoformulations of imazamox for minimizing environmental risk

Rachid Khatem[a], Rafael Celis[b], M. Carmen Hermosín[b,*]

[a] *Laboratory of Biodiversity and Conservation of Soil and Water, University of Abdelhamid Ibn badis Mostaganem, Algeria*

[b] *Instituto de Recursos Naturales y Agrobiología de Sevilla, Consejo Superior de Investigaciones Científicas (IRNAS, CSIC), Spain*

Number of pages: 8

Number of tables: 3

Number of figures: 4

Table S1

Physicochemical properties of the soil sample used in the study.

Textural class	Sand (%)	Silt (%)	Clay (%)	$CaCO_3$ (%)	OC[a] (%)	pH[b]
Sandy loam	80.3	7.1	12.6	5.6	0.9	8.2

[a] Organic carbon.

[b] pH measured in a 1:2 soil/water suspension.

Table S2

Instrumental conditions for the analysis of imazamox by HPLC.

Instrument	Waters 600E chromatograph
Column	Nova-Pak C18 column, 150 mm length × 3.9 mm i.d.
Detector	PDA detector Waters 996, λ= 245 nm
Flow rate	1 mL min^{-1}
Mobile phase	Acetonitrile:H_3PO_4 aq. pH 2, 20:80 (v/v)
Injection volume	25 µL
Analysis time	6 min
Retention time	3.5 min

Table S3

Constants from fitting the modified Fickian kinetic equation: $M_t/M_z = k \cdot t^n + c$ to the release data of imazamox in water for the free technical product and Imz-clay complexes.

	k	***n***	***c***	R^2
Technical Imz (free)	1.45 ± 0.35	0.056 ± 0.033	98.2 ± 0.3	0.917
Imz-LDH RE	9.28 ± 2.00	0.171 ± 0.033	67.4 ± 1.9	0.935
Imz-LDH DS	0.76 ± 0.53	0.517 ± 0.136	64.5 ± 0.8	0.934
Imz- Clo10A SC	3.01 ± 1.40	0.208 ± 0.076	85.4 ± 1.4	0.810
Imz- Clo10A WC	2.59 ± 2.78	0.305 ± 0.186	72.1 ± 2.9	0.663
Imz-Clo10A GM	2.03 ± 1.32	0.190 ± 0.101	93.8 ± 1.2	0.658

Discussion: The high value of *c* obtained for technical Imz reveals the high immediate release by dissolution of the herbicide. The lowest values of *c* and *k* correspond to Imz-LDH DS, confirming the low initial release and release rate of Imz from this formulation. The best controlled release profile is shown by Imz-LDH RE, with a *c* value of 67% and a release constant *k*= 9.28. The Imz-Clo10A complexes give intermediate *k* values, which were similar for the three prepared complexes, as indicated by the release profiles. The slow release performance of the complexes decreased in the order: Imz-LDH RE > Imz-Clo10A SC > Imz-Clo10A WC > Imz-Clo10A GM > Imz-LDH DS.

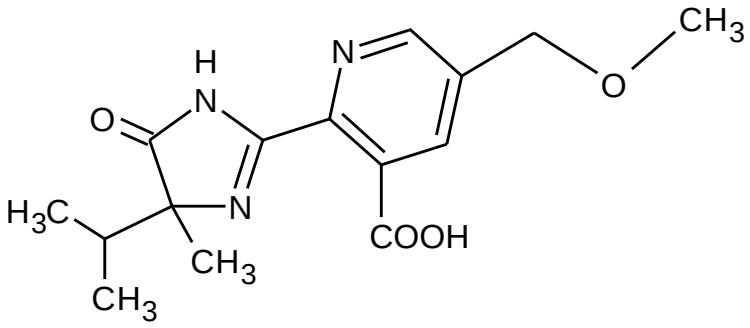

Fig. S1. Chemical structure of Imazamox.

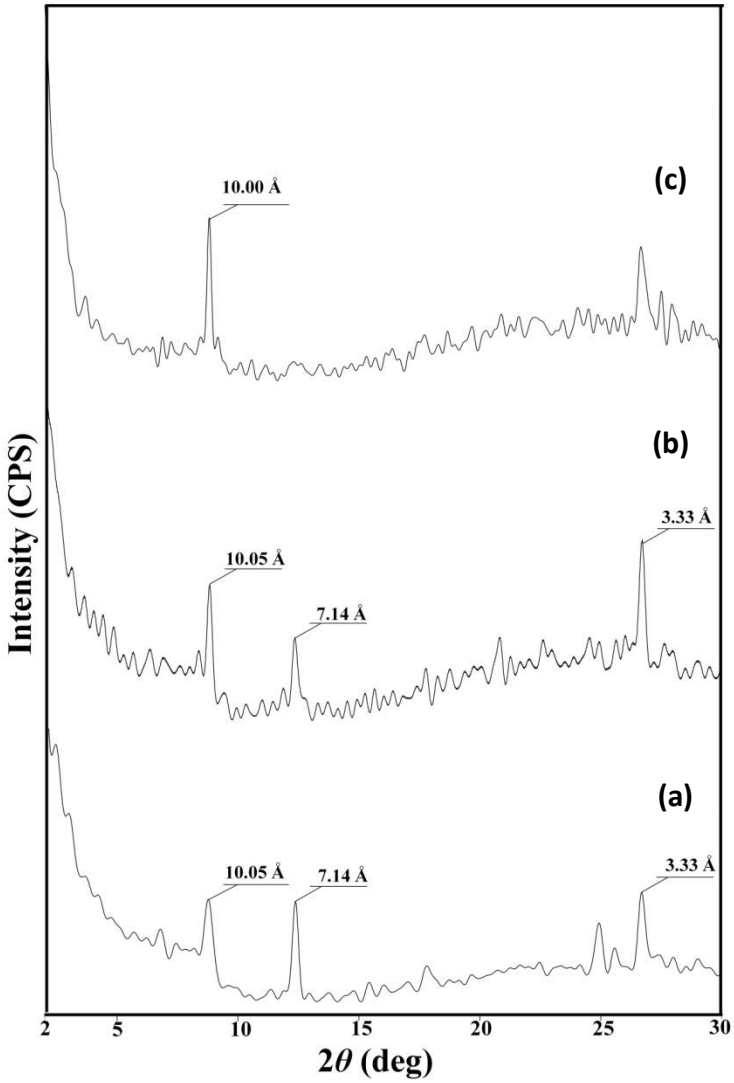

Fig. S2. X-ray diffractograms of the clay (< 2 μm) fraction of the soil subjected to different treatments: (a) saturated with Mg^{2+}, (b) saturated with K^{+}, (c) saturated with K^{+} and heated at 500 ºC. Reflections at 10.05 and 7.14 Å in (a) and (b) and disappearance of the 7.14 Å-reflection in (c) indicate the predominance of illite/mica and kaolinite in the sample.

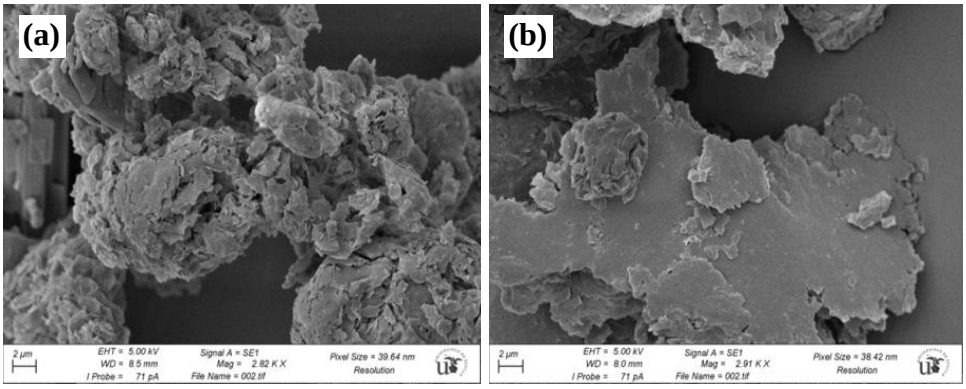

Fig. S3. Scanning electron micrographs of: (a) Imz-Clo10A GM and (b) Clo10A shaken in methanol for 24 h (control for Imx-Clo10A SC).

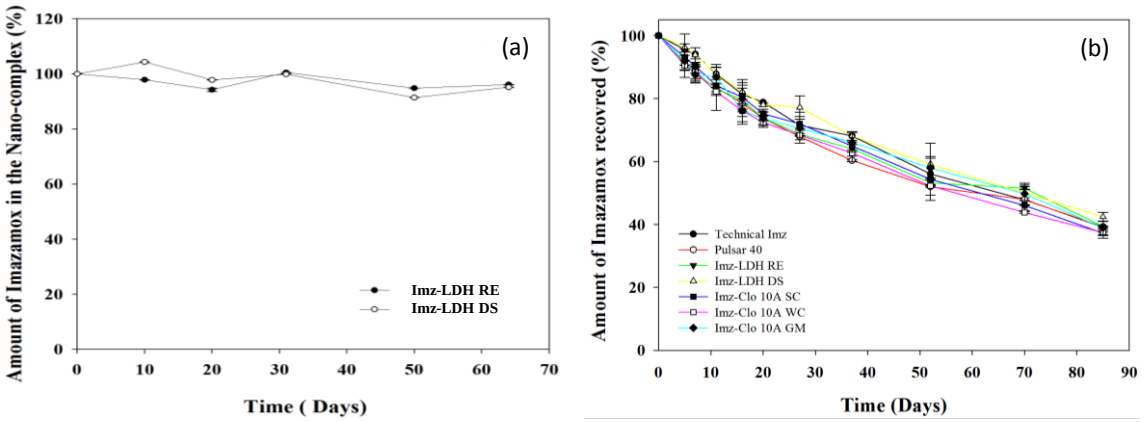

Fig. S4. (a) Stability curves for the Imz-LDH complexes and (b) Dissipation curves for technical imazamox, commercial imazamox (Pulsar 40) and the nano-formulations in soil.